11. Injector

11.1 Introduction

Storage of a stable beam of electrons in the main ring must be preceded by their generation and acceleration. To this end, two additional accelerators connected in series, called the injection system, must be provided. In our case we propose that we can use the pre-injector and the booster synchrotron of BESSY I without any major changes.

Naturally, the electrons must be successively delivered from one accelerator to the next one. Because the lattices of the various accelerators are very different, i.e. each machine has its own equilibrium emittances; it is necessary to couple them appropriately so that an optimal beam transfer can occur. For the transfer line between the pre-injector and the booster synchrotron we are willing to keep it unchanged but we need a new transfer line from the booster to the storage ring and we intend to make use of as many elements as possible from the existing elements of the old transfer line in our design.

The successive injections are designed to take place in the horizontal plane; in order to save space the whole injector is inside the storage ring. The slow injection system from the pre-injector to the booster as well as the slow extraction system from the booster will not change. For injection to the storage ring we need to design a fast injection system because we want to accumulate. On the other hand because our storage ring is a compact one, we don't have any long enough straight section to place all the injection elements. Therefore, we have to think about other possibilities; for instance an injection scheme consisting of 3 kickers distributed in three successive high beta sections.

In the following sections, we first introduce the specifications of the microtron and the booster synchrotron, then we describe the transfer line to the storage ring and finally the injection elements and injection scheme to the storage ring are discussed.

11.2 Microtron

The preinjector of BESSYI was a 20 keV classical microtron. The characteristics of this microtron are listed in Table (11.1).

Table 11.1:Characteristics of the microtron

Extractable energy , MeV	22.5
Energy gain per turn , keV	535
Energy spread (FWHM), keV	35
Magnetic field , T	0.112
Magnet diameter , m	2.22
Pole piece diameter , m	1.8
Gap height , m	0.11
Magnet width , m	0.45
Microwave frequency , GHz	3.0
Microwave peak power , MW	2
Pulse duration , μs	4
Pulse repetition rate , Hz	≤ 250
Working vacuum , $mbar$	10^{-6}
Pulse current , mA	15
Vertical emittance , $\mu mrad$	≤ 8
Horizontal emittance , $\mu mrad$	≤ 3

As has been mentioned in the Green book, this microtron contributed dominantly to the total failure rate of the accelerator facility. The problems are mentioned there, but after a thorough refurbishment the microtron may still be used as a pre-injector. For future upgrades using a linac could be proposed.

11.3 Booster Synchrotron

The booster synchrotron has a six fold symmetry with a substructure for each of F B D B F, see Figure (11.1).

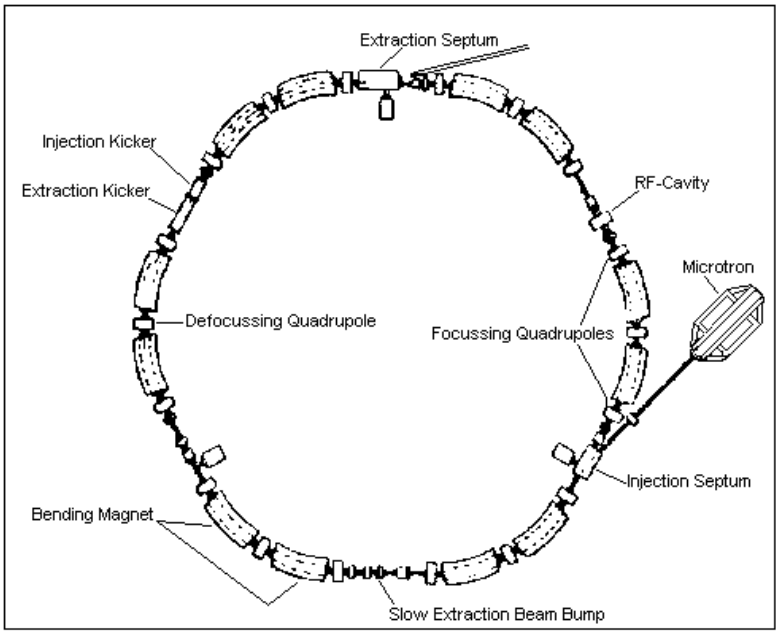

Figure 11.1:Layout of the booster synchrotron and the microtron

The unit cell and the main optical functions are shown in Figure (11.2) and Figure (11.3). For more detailed description there is a good reference [1]. The characteristics of the booster are also listed in Table (11.3). As changes only there will be a different philosophy of powering magnets, instead of White circuits of the BESSY I we will use ramping power supplies with $1\,Hz$ repetition rate. At energy 776 (MeV) a value of 7 ($mA/shot$) has already been reached at BESSY I. Therefore, even with one shot per second the filling time of the storage ring will be a few minutes. In Table (11.2) the lattice of the booster is shown.

Table 11.2: Lattice of booster synchrotron, the super periodicity is six

Name code	Element	Length, (m)	$\rho,(m)$	$k,(m^{-2})$	$s,(m)$
1	D1	1.025			1.025
2	QF	0.25		1.69	1.275
3	D2	0.21			1.485
4	rB	1.398	2.67		2.883
5	D2	0.21			3.093
6	QD	0.25		-1.53	3.343
7	D2	0.21			3.553
8	rB	1.398	2.67		4.951
9	D2	0.21			5.161
10	QF	0.25		1.69	5.411
11	D1	1.025			6.436

Table 11. 3: Characteristics of the booster

Maximum energy , MeV	800
Injection energy , MeV	20
Circumference , m	38.58
Superperiodicity	6
Number of bending magnets	12
Number of focussing quadrupoles	12
Number of defocusing quadrupoles	6
Repetition rate , Hz	1
Horizontal tune , Q_x	2.22
Vertical tune , Q_y	1.31
Momentum compaction factor α	0.18
Harmonic number	64
RF-frequency , MHz	500
RF-output power , kW	2
Cavity shunt impedance , $M\Omega$	3
Current @maximum energy , mA	7
Vertical emittance , $\mu mrad$	0.016
Horizontal emittance , $\mu mrad$	0.155

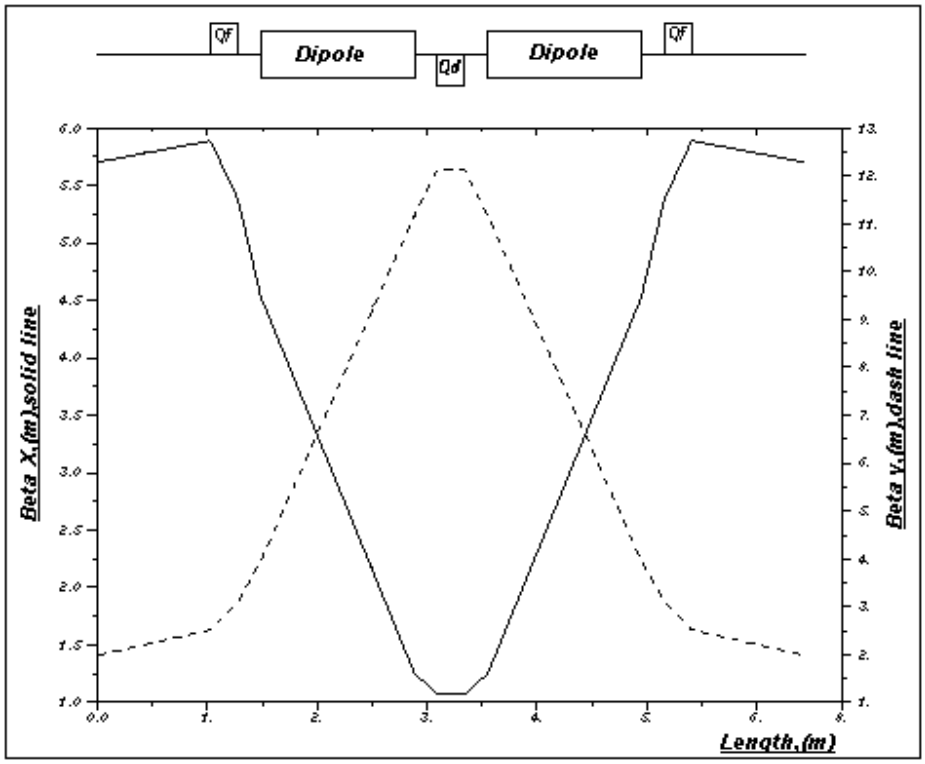

Figure 11.2: Beta functions versus position in one cell of the booster synchrotron consisting of two bending magnets and three quadrupoles

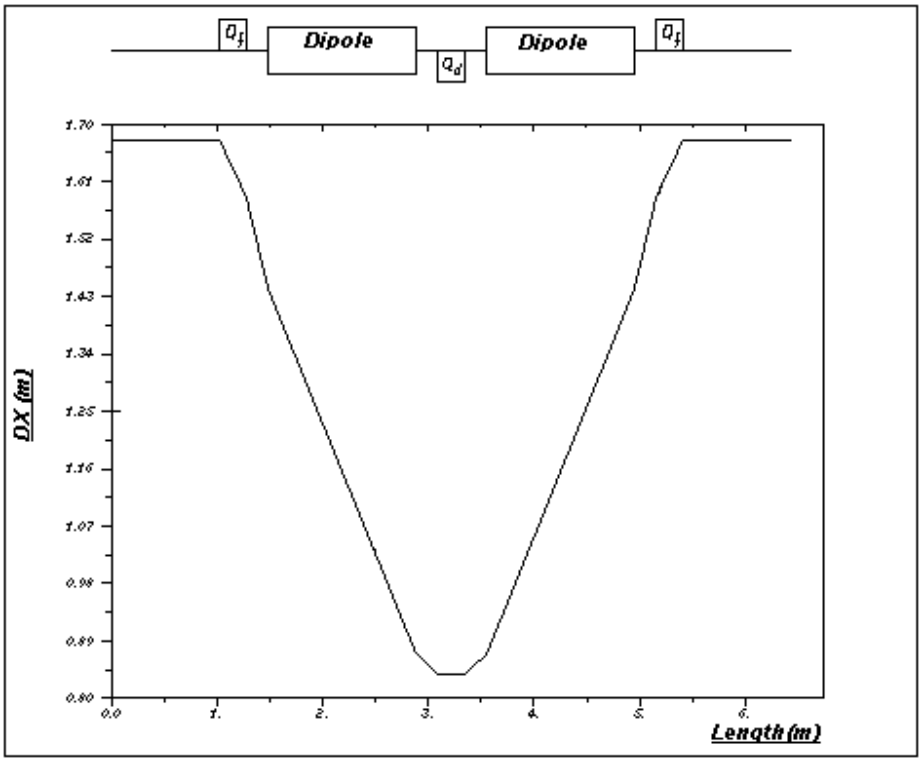

Figure 11.3: Horizontal dispersion function versus position in one cell of the booster synchrotron consisting of two bending magnets and three quadrupoles

11.4 Transfer Line

The transfer line of BESSYI cannot any longer be used and the reasons are: totally different storage ring and the fact that at BESSY I the injector was outside the storage ring and vertical injection was used. Therefore in our case we need a new transfer line. This transfer line has been designed based on using as many elements as possible from existing elements of the old transfer line.

In calculations we started with the extraction septum of the booster and we ended up with the injection septums. As the end of the transfer line, one high beta section of the storage ring, we did a calculation for (SES_4_1_1) according to notation of (3.3.2.3), see also Table (11.6). In the vicinity of the storage ring there are many geometrical limitations coming from the philosophy of putting the injector inside the storage ring whilst we don't like to use a very strong injection septum. Also we like to keep the flexibility of this transfer line as much as possible. In fact, the designed transfer line is working for main mode (full match in horizontal and vertical planes) and also its functionality has been checked for a variety of mismatches; Table (11.4) shows the results of these calculations. In each column there is some settings for quadrupoles that give the desired set of optical values. In this table the first column shows the values for the main mode. As with ANKA one can think about beta mismatches and the possible increase in the injection efficiency [2]. These settings are described in the next eight columns. The last two columns are the results for dispersion mismatching. Therefore this transfer line could make, more or less, any reasonable setting. All *K*-values of the quadrupoles are between *–4* and *4* $(1/m^2)$, and we know that *g*-factor of quadrupoles of BESSYI is $12\,(T/m)$ and the energy of particles in transfer line is $800\ (MeV)$. Therefore, any value between *–4.4* and *4.4* for *K*-value of quadrupoles is allowed. Also except than some extreme cases the minimum values of the beta functions are acceptable.

Table 11.4: Flexibility checks for the transfer line

$\beta_x(m)$	**13.6**	13.6	13.6	7	7	7	27	27	27	8	8
$\beta_y(m)$	**2.72**	5.4	1.4	2.7	5.4	1.4	2.7	5.4	1.4	2.72	2.72
D_x	**0.51**	----	----	----	----	----	----	----	----	1	0
$Q1[K1]$	**-2.67**	-2.68	-2.23	-2.57	-2.9	-2	-3	-2.9	-3.255	**-4**	1.64
$Q2[K1]$	**1.98**	1.97	1.61	2.12	2.17	1.79	1.7	1.64	1.43	3.38	-2.38
$Q3[K1]$	**3.04**	3	2.52	3.07	3.13	2.9	2.85	3.2	2.786	2.24	0.83
$Q4[K1]$	**-1.84**	-1.83	-0.94	-1.82	-1.7	-1.7	-1.297	-1.86	-1.27	-1.32	1.47
$Q5[K1]$	**-3.07**	-3.33	-3.22	-3.03	-3	-3.1	-2.98	-2.5	-3.107	-3.28	-3.98
$Q6[K1]$	**2.87**	2.85	2.92	3.36	3.49	3.23	2.41	2.27	2.04	2.88	**3.86**
$\beta_{x,\max}$	**17.3**	17.7	17.3	13.6	16.8	11.4	28.7	28.3	42.4	11.4	15.1
$\beta_{x,\min}$	**1.67**	1.3	1.22	2.7	3.2	2	1	1.5	0.3	1.37	0.7
$\beta_{y,\max}$	**12.1**	11.5	19	16.6	13.8	23.3	12.3	9.5	17.8	10.3	12
$\beta_{y.\min}$	**1.51**	0.8	1.38	1.98	1.98	1.4	1.98	1.98	1.2	1.6	1.9

As any other transfer line well behavior optical functions were desired and has been achieved. Figures (11.4) - (11-5) show main mode's optical functions. The variation of σ_x is shown in Figure (11.6).

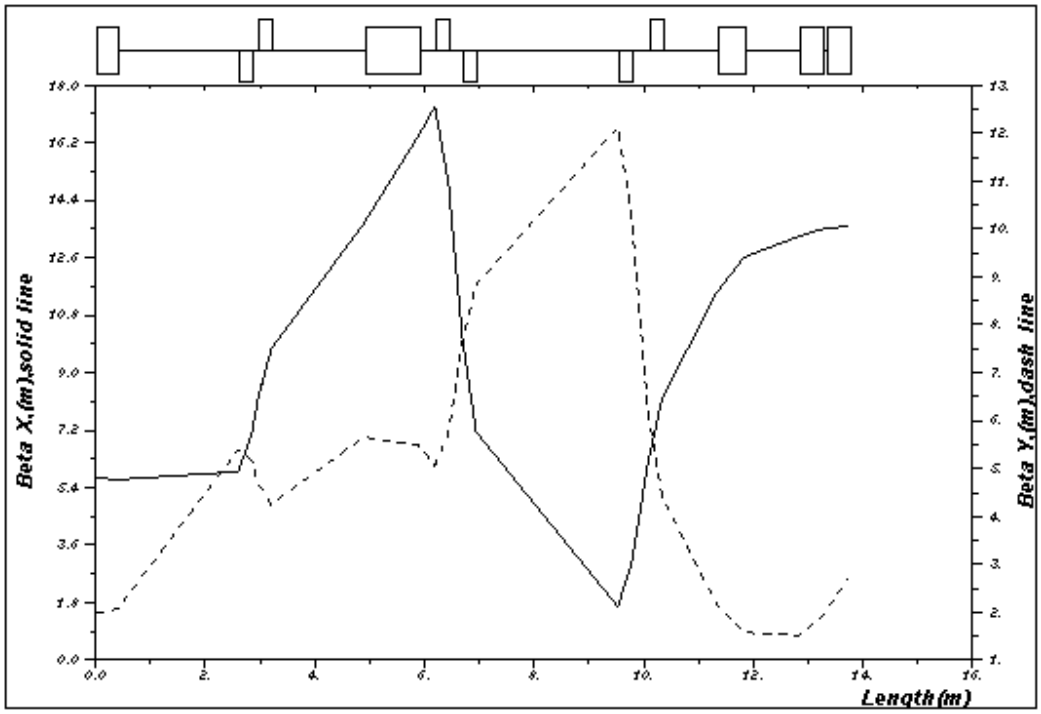

Figure 11.4: Horizontal and vertical beta functions versus position in the transfer line for full matching of machines optical functions

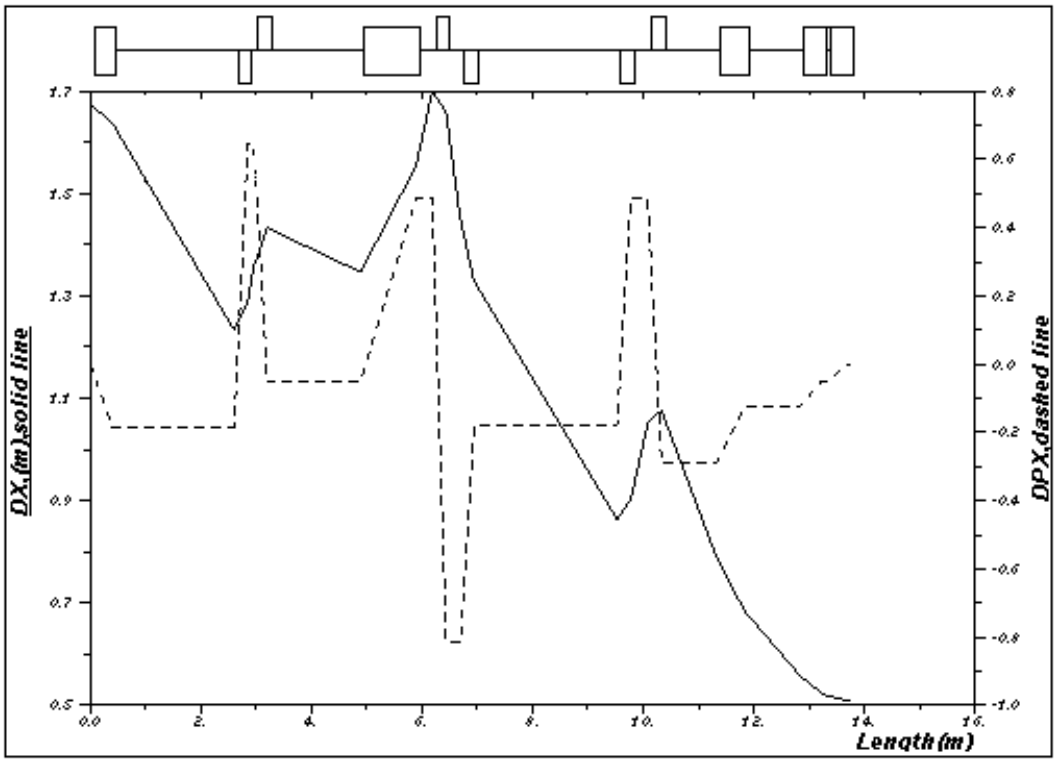

Figure 11.5: Horizontal dispersion function and its derivative as a function of position in the transfer line

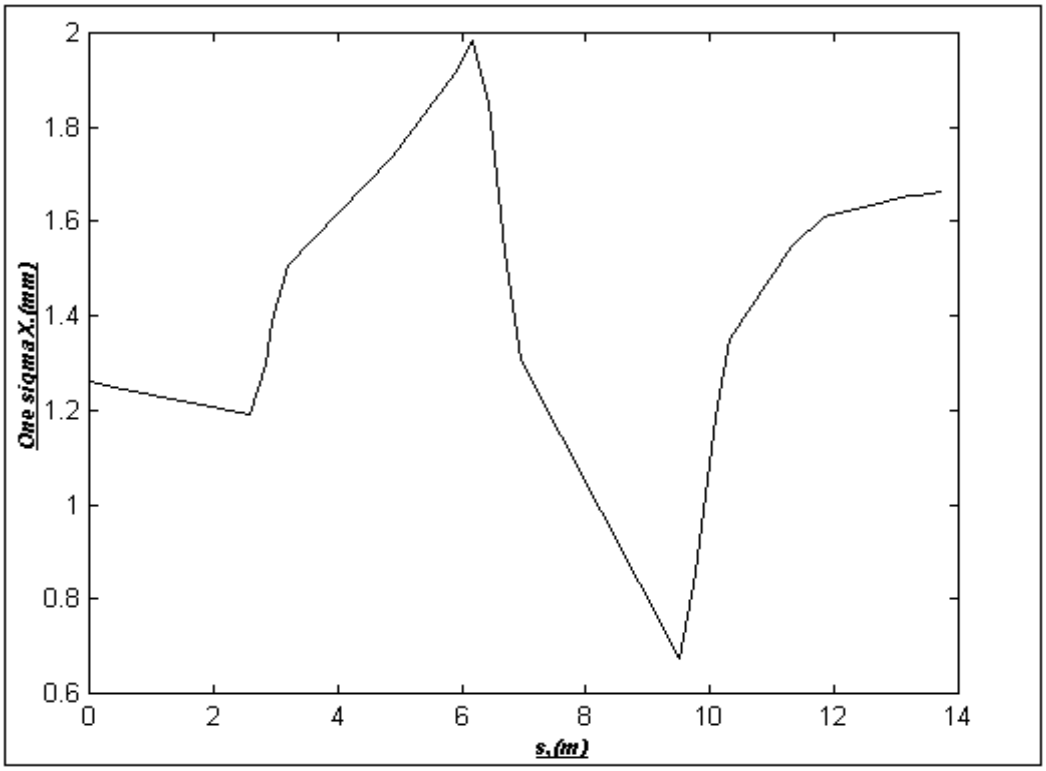

Figure 11.6: Horizontal beam half width, σ_x, and its variation in the transfer line for full match

In Table (11.5) we list the lattice of the transfer line. Table (11.6) contains lattice of the storage ring, which is used in the calculations of this section.

Table 11.5: Lattice of the transfer line

Name code	Element	Length, (m)	$\rho,(m)$	$k,(m^{-2})$	$s,(m)$
1	Sep-ej	0.4	3.276		0.4
2	D1	2.2			2.6
3	Q1	0.25		-2.67	2.85
4	D2	0.105			2.955
5	Q2	0.25		1.98	3.205
6	D3	1.678			4.883
7	rB1	1	1.91		5.883
8	D4	0.303			6.186
9	Q3	0.25		3.04	6.436
10	D5	0.254			6.69
11	Q4	0.25		-1.84	6.94
12	D6	2.58			9.52
13	Q5	0.25		-3.07	9.77
14	D7	0.308			10.078
15	Q6	0.25		2.867	10.328
16	D8	1			11.328
17	rB2	0.5	1.91		11.828
18	D9	1			12.828
19	Sep-in2	0.4	4.582		13.228
20	D10	0.1			13.328
21	Sep-in1	0.4	7.619		13.728

Table 11.6: One superperiod of the storage ring, the superperiodicity is eight

Name code	Element	Length, (m)	$\rho,(m)$	$k,(m^{-2})$	$m,(m^{-3})$	$s,(m)$
1	D1	1.5				1.5
2	SF	0.15			14.89	1.65
3	D2	0.15				1.8
4	QF1	0.24		2.786		2.04
5	D3	0.25				2.29
6	SD	0.15			-19.8	2.44
7	D4	0.1				2.54
8	QD	0.12		-2.56		2.66
9	D5	0.2				2.86
10	rB	1.94	4.9427	-0.341		4.8
11	D5	0.2				5
12	SD	0.15			-19.8	5.15
13	D6	0.25				5.4
14	QF2	0.24		2.635		5.64
15	D2	0.15				5.79
16	SF	0.15			14.89	5.94
17	D7	1.559				7.499
18	D7	1.559				9.058
19	SF	0.15			14.89	9.208
20	D2	0.15				9.358
21	QF2	0.24		2.635		9.598
22	D6	0.25				9.848
23	SD	0.15			-19.8	9.998
24	D5	0.2				10.198
25	rB	1.94	4.9427	-0.341		12.138
26	D5	0.2				12.338
27	QD	0.12		-2.56		12.458
28	D4	0.1				12.558
29	SD	0.15			-19.8	12.708
30	D3	0.25				12.958
31	QF1	0.24		2.786		13.198
32	D2	0.15				13.348
33	SF	0.15			14.89	13.498
34	D1	1.5				14.998

In Figure (11.7) a drawing of the whole transfer line with the elements of the injection straight section is shown. For instrumentation of this transfer line some elements are predicted; Table (11.7) and Figure (11.7). Thus by using some elements of the old transfer line we can do the job of transferring the beam to the storage ring and only we need two new septums and a new small bending magnet; Table (11.8).

Table 11.7: Instrumentation of the transfer line

Element	Number
F.C.T	1
Scraper	1
Screen monitors	3

Table 11.8: Elements of the transfer line and their status

Element	Number	Status
Quadrupoles and their power supplies	6	Available from BESSYI
Steerers and their power supplies	12	Available from BESSYI
Main bending magnet	1	Available from BESSYI
Small bending magnet	1	Not available from BESSYI
Extraction septum	1	Available from BESSYI
Injection Septums	2	Not available from BESSYI

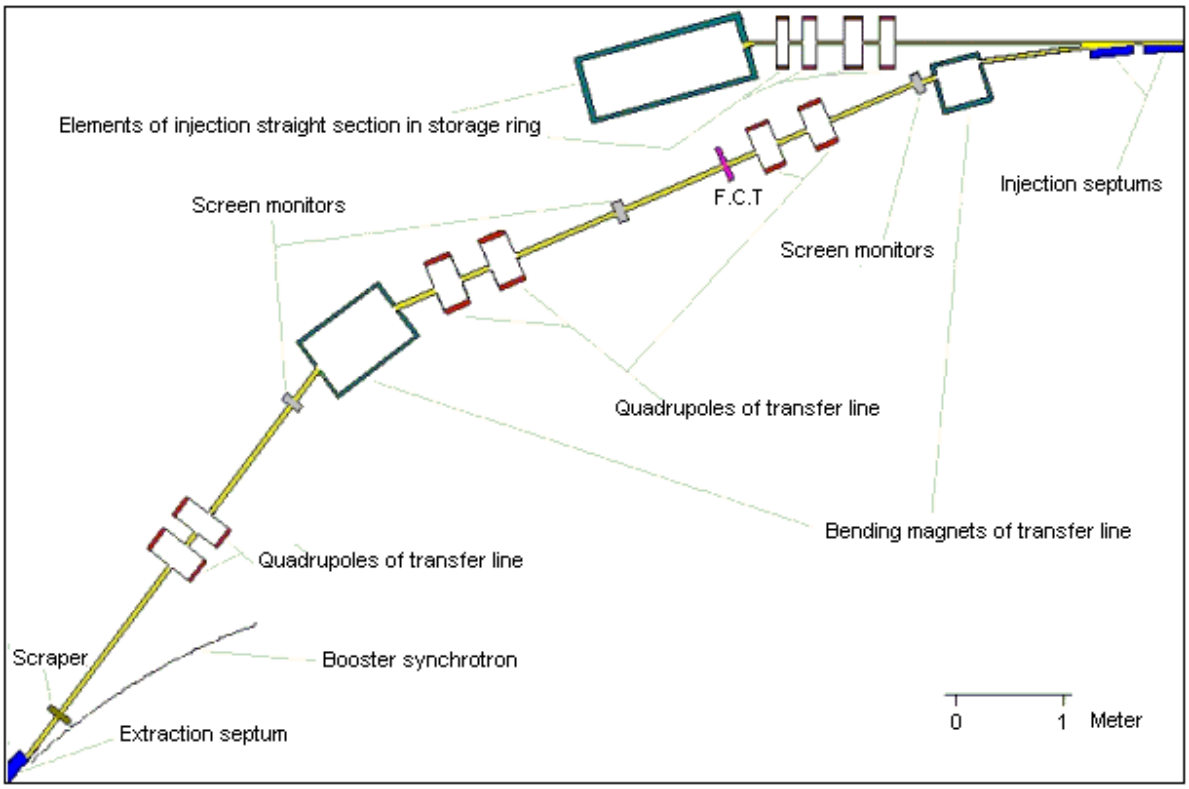

Figure 11.7: The transfer line and its elements and their arrangement with respect to the booster and the storage ring

11.5 Injection to the Storage Ring

As mentioned in 11.1, we have to distribute the injection elements over several successive straight sections, like what implemented for ANKA and MAXII, [2] and [3]. In the following we present the results of the first studies for this purpose. This study had several steps:

1. Optimization of places of the kickers by demanding minimum strength for kickers whilst keeping some geometrical limitations served
2. Investigating the effect of sextupoles on the injection bump, and making necessary correction to close this bump
3. Injection efficiency studies and simulation of injection process

11.5.1 Optimization of the Places of the Kickers

In order to make a closed orbit bump by three kickers there is a well-known set of equations for strengths of kickers, Equations (11.1) – (11.3). These kicker strengths, θ_1, θ_2 and θ_3 are dependent on the deviation from reference orbit, B, phase advances, $\Delta\psi$, and values of optical functions, β. The indexes 1, 2, 3, s stand for kicker1, kicker2, kicker3 and septum respectively. According to this relations and after some simple algebra one can conclude that for a definite B the minimum strengths are in the arrangement (1,2,3) of Figure (11.8), but coming from lack of existing space for our kickers we would rather to use scheme $(1, 2', 3)$.

$$\theta_1 = B/(\sqrt{\beta_1\beta_s}\,Sin\,\Delta\psi_{s1}) \qquad (11.1)$$

$$\theta_2 = -BSin\Delta\psi_{31}/(\sqrt{\beta_2\beta_s}\;\; Sin\Delta\psi_{32}\;Sin\Delta\psi_{s1}) \qquad (11.2)$$

$$\theta_3 = BSin\Delta\psi_{21}/(\sqrt{\beta_3\beta_s}\;\; Sin\Delta\psi_{32}\;Sin\Delta\psi_{s1}) \qquad (11.3)$$

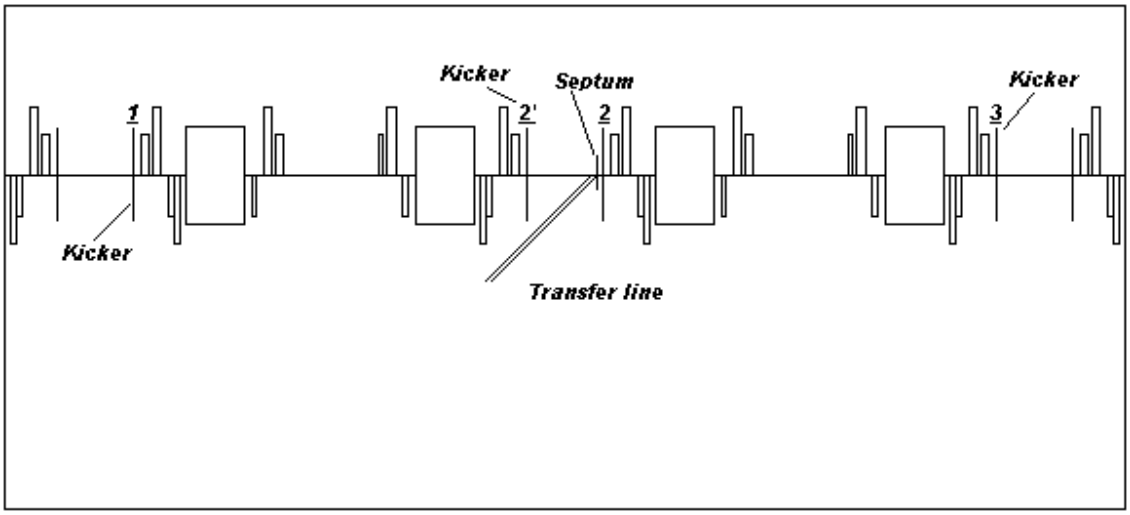

Figure 11.8: Three high beta sections of the storage ring with two low beta sections in between. Kickers are placed in high beta sections as red lines, each combination of three selection, one from each section is an alternative but the best one is (1,2,3) and because of geometrical limitation we will use (1,2', 3).

11.5.2 Effect of Sextupoles

The simple argument of previous section gave us the best injection scheme, but because our kicked orbit is passing through sextupoles with some definite deviation, it will sense some additional kicks. In Figure (11.9) the result of this simple closed orbit bump is shown for the two

cases of sextupoles on and off. Apparently the bump is not closed. There is a variation method provided by MAD and there one can make necessary correction to close this bump empirically. In Figure (11.10) the result after this correction is presented. Also the reduced strengths for kickers are mentioned.

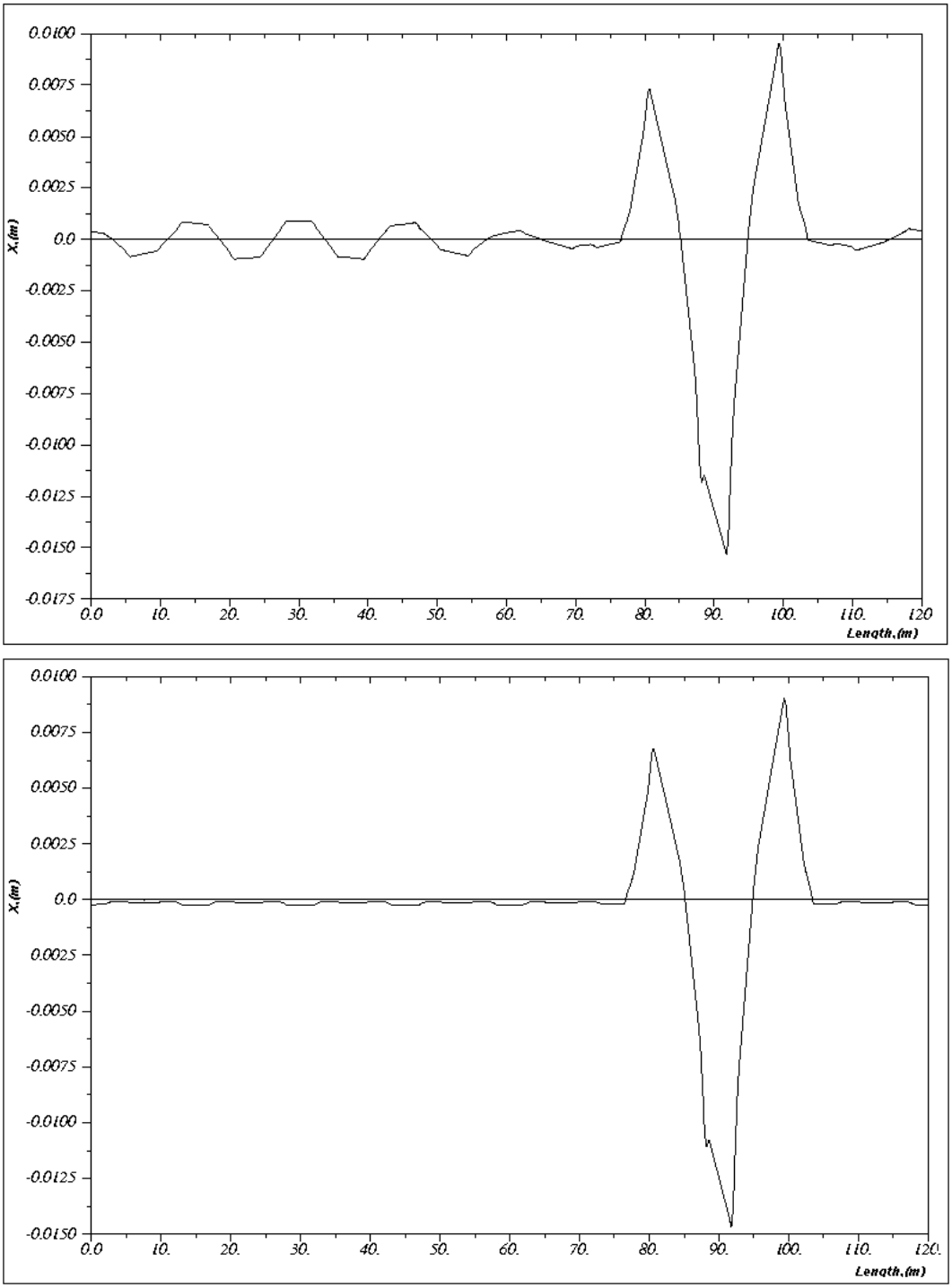

Figure 11.9: The horizontal orbit in the whole machine with active kickers. The strengths are according to simple Equations (11.1) – (11.3). At the top sextupoles are On while they are Off at the bottom. The strengths are 1.13, -2.12 and 1.5 (*mrad*) for kickers 1,2', 3 of Figure (11.8) respectively.

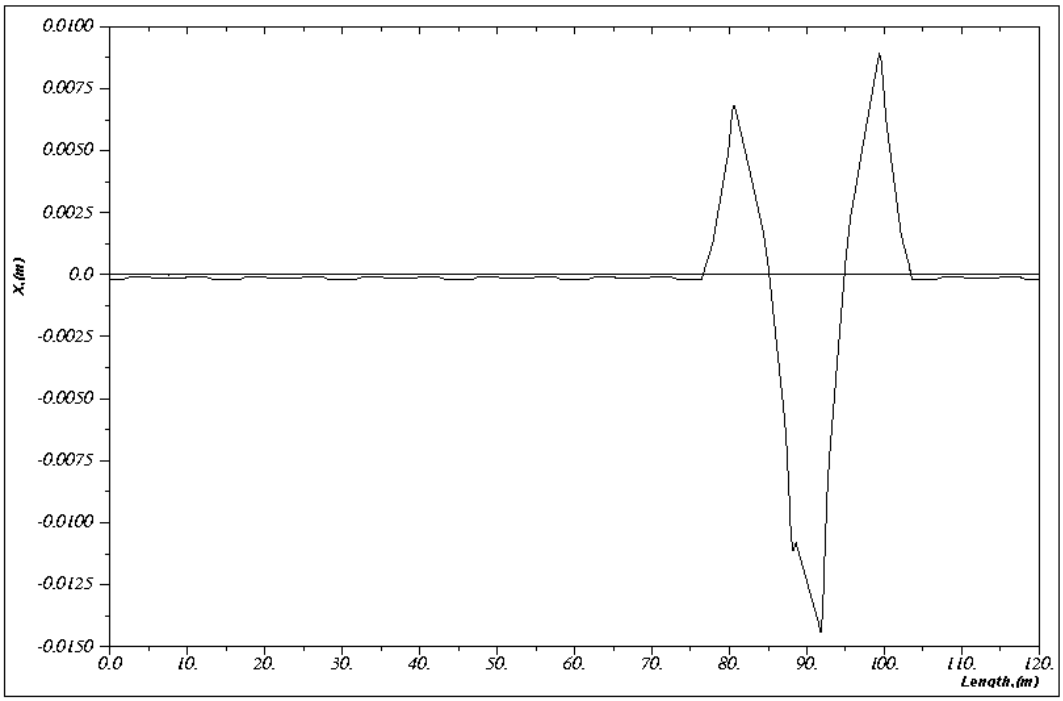

Figure 11.10: Corrected injection bump. The strengths are 1.13, -1.98 and 1.47 (*mrad*)

11.5.3 Injection Efficiency Studies and Simulation of Injection Process

In this part of study we should be able to introduce any required distribution of particles at the place of injection septum. Also for optimizing the pulse of kickers (width and phase) we need to be able to introduce fast elements i.e. kickers to our simulator.

The circumference of our storage ring is $400\,n\sec$ (in time domain) and as the characters of activating pulse for kickers, similar to ANKA, we started with $3\,\mu\sec$ pulse width and half-sinusoidal variation. Technically these parameters seem to be easy to achieve remembering relatively low required kicker strengths of Figure (11.10). With these characters if we inject at the crest of the pulse, in addition to main kicks, the orbit will face three weaker series of kicks. Certainly this is what we must study carefully. The values of the tunes have their own role too. Also geometrical limits should be taken into account, especially the cross section of the vacuum chamber at the place of the septum. Coming from all these considerations we can not expect a good injection efficiency in the case of injecting at the crest of the activating pulse of the kickers, because at the very end series of kicks the injected particles will hit to septum sheet. One way is to inject one turn after crest, Figure (11.11). Then the injected particles will face totally *3* series of kicks, and they will survive to all conditions. Another way is to use faster kickers. If we decrease the pulse width to *2.1* $\mu\sec$ then the total number of coincidence of particles and active kickers will be three, hence there is more chance to accumulate the injected particles. In Figure (11.12) the result of tracking with active kickers for $3\,\mu\sec$ is shown. As said before they are injected one turn after the crest. We introduced four particles sitting at the four major vertexes of the injected envelope of $2.2\sigma_x$ and $5\sigma_{x'}$ major and semimajor diameters. Rigth after injection they will face kickers $3,1,2'$ of Figure (11.8) respectively. Then they will go to position 1 of Figure (11.12). Now by facing next complete chain of kicks they will go to position 2 and for the third time after kicker 3 when they arrive to position of kicker 1 the kickers are off. One should continue this tracking for some definite turns with the kickers turned off. Only in this case we can be sure that our particles are survived. In

Figure (11.13) the result of tracking for *200* turns after the action of kickers is presented. Before 20 turns there is no good knowledge about the required physical aperture.

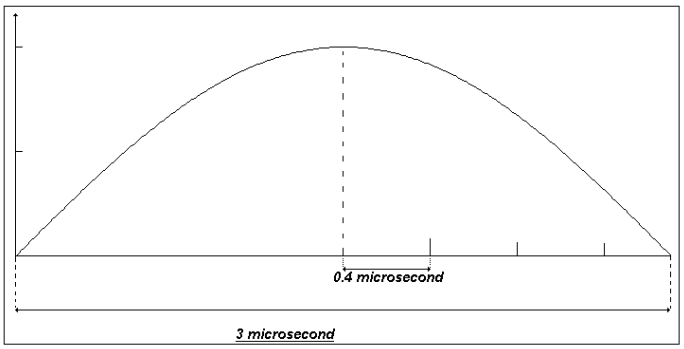

Figure 11.11: Activating pulse of the kickers

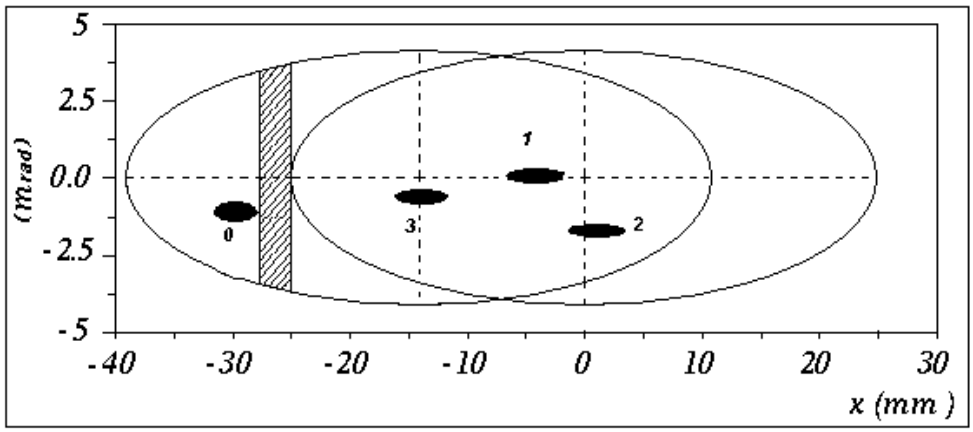

Figure 11.12: Injected beam and its movement in phase space at the injection point

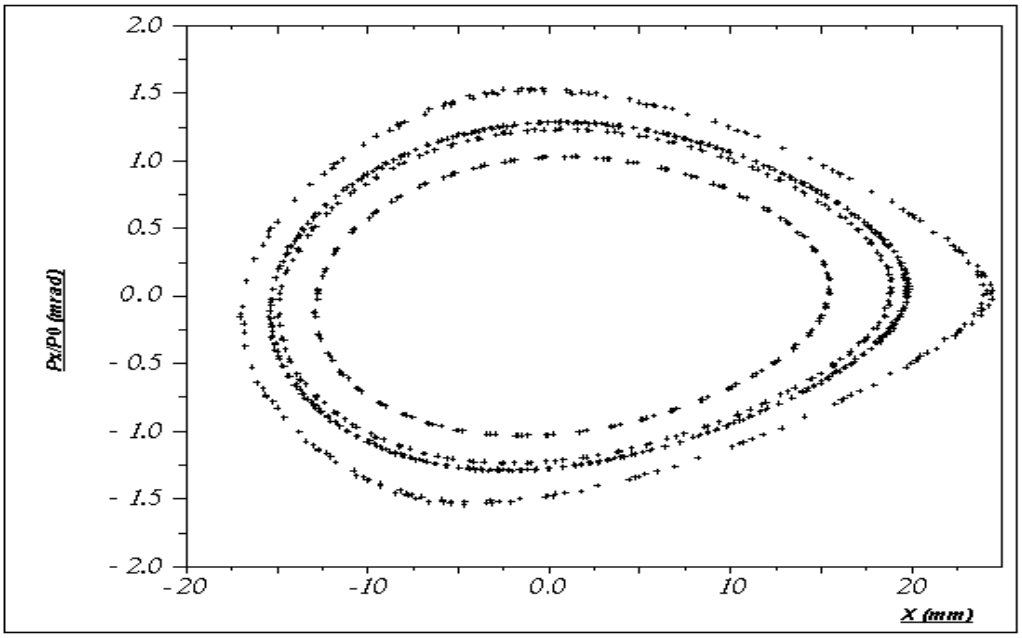

Figure 11.13: The particles of Figure (11.11) are survived in the physical aperture of the machine

According to the results of tracking, the position acceptance is $2.2\sigma_x$ and the angle acceptance is $5\sigma_{x'}$. Therefore, with characters of kickers according to Table (11.9) we can expect acceptable injection efficiency, near *%70*. There are possibilities to make some kind of mismatches to gain more from injected beam. These kinds of mismatches are still under study.

Table 11.9: Elements required for injection to the storage ring

Injection elements	Number	Length, (cm)	Pulse width, half sinusoidal (μsec)	Strength $(mrad)$
Kicker	3	20	3	~2
Septum	1	40	250	60
Septum	1	40	250	90

In Tables (11.10) and (11.11) the elements of the injection straight sections and their characters are listed.

Table 11.10: Lattice of Line named "PA" in Table 11.11

Name code	Element	Length, (m)	$\rho,(m)$	$k,(m^{-2})$	$m,(m^{-3})$	$s,(m)$
1	SF	0.15			14.89	015
2	D2	0.15				0.3
3	QF1	0.24		2.786		0.54
4	D3	0.25				0.79
5	SD	0.15			-19.8	0.94
6	D4	0.1				1.04
7	QD	0.12		-2.56		1.16
8	D5	0.2				1.36
9	rB	1.94	4.9427	-0.341		3.3
10	D5	0.2				3.5
11	SD	0.15			-19.8	3.65
12	D6	0.25				3.9
13	QF2	0.24		2.635		4.14
14	D2	0.15				4.29
15	SF	0.15			14.89	4.44
16	D7	1.559				5.999

Table 11.11: Structure of the injection lattice

Name code	Element	Length, (m)	Strength $(mrad)$	s, (m)
1	KIK 1		1.1345	0
2	D1	0.075		0.075
3	**PA,-PA**	11.998		12.073
4	D2	0.075		12.148
5	KIK 2		-1.978	12.148
6	D3	2.825		14.973
7	SEPTUM			14.973
8	D4	0.1		15.073
9	**PA,-PA**	11.998		27.071
10	D5	0.075		27.146
11	KIK 3		1.471	27.146
12	D6	2.925		30.071
13	**PA,-PA**	11.998		42.069
14	D7	1.5		43.569

Reference

[1] G. v. Egan-Krieger, D. Einfeld, W.- D. Klotz, H. Lehr, R. Maier, G. Mulhaupt, R. Richter and E. Weihreter, *"PERFORMANCE OF THE 800 MeV INJECTOR FOR THE BESSY STORAGE RING"*.

[2] D. Einfeld, S. Hermle, E. Huttle, R. Rossmanith, R. Walther, "*THE INJECTION SCHEME FOR THE ANKA STORAGE RING*".

[3] Greg LeBlanc and Lars-Johan Lindgren, "*The Injection Scheme for the New 1.5 GeV Storage Ring, MAX-II"*.